



Crystallization and X-ray analysis of D-threonine aldolase from *Chlamydomonas reinhardtii*

Yuki Hirato, Masaru Goto, Mayumi Tokuhisa, Minoru Tanigawa and Katsushi Nishimura

Acta Cryst. (2017). F73, 86–89



IUCr Journals

CRYSTALLOGRAPHY JOURNALS ONLINE

Copyright © International Union of Crystallography

Author(s) of this paper may load this reprint on their own web site or institutional repository provided that this cover page is retained. Republication of this article or its storage in electronic databases other than as specified above is not permitted without prior permission in writing from the IUCr.

For further information see <http://journals.iucr.org/services/authorrights.html>

Crystallization and X-ray analysis of D-threonine aldolase from *Chlamydomonas reinhardtii*

Yuki Hirato,^a Masaru Goto,^b Mayumi Tokuhsa,^a Minoru Tanigawa^a and Katsushi Nishimura^{a,c,*}

^aDepartment of Materials and Applied Chemistry, College of Science and Technology, Nihon University, 1-8-14 Kanda-Surugadai, Chiyoda-Ku, Tokyo 101-8308, Japan, ^bDepartment of Biomolecular Science, Faculty of Science, Toho University, 2-2-1 Miyama, Funabashi, Chiba 274-8510, Japan, and ^cDepartment of Biotechnology and Material Chemistry, Junior College, Nihon University, 7-24-1 Narashinodai, Funabashi, Chiba 274-8501, Japan. *Correspondence e-mail: nishimura.katsushi@nihon-u.ac.jp

Received 15 November 2016

Accepted 29 December 2016

Edited by A. Nakagawa, Osaka University, Japan

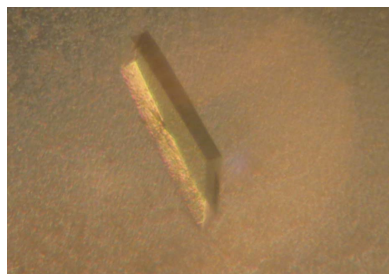
Keywords: D-threonine aldolase; *Chlamydomonas reinhardtii*; D-amino acids; crystallization.

D-Threonine aldolase from the green alga *Chlamydomonas reinhardtii* (CrDTA) catalyzes the interconversion of several β -hydroxy-D-amino acids (e.g. D-threonine) and glycine plus the corresponding aldehydes. Recombinant CrDTA was overexpressed in *Escherichia coli* and purified to homogeneity; it was subsequently crystallized using the hanging-drop vapour-diffusion method at 295 K. Data were collected and processed at 1.85 Å resolution. Analysis of the diffraction pattern showed that the crystal belonged to space group *P*1, with unit-cell parameters $a = 64.79$, $b = 74.10$, $c = 89.94$ Å, $\alpha = 77.07$, $\beta = 69.34$, $\gamma = 71.93^\circ$. The asymmetric unit contained four molecules of CrDTA. The Matthews coefficient was calculated to be $2.12 \text{ \AA}^3 \text{ Da}^{-1}$ and the solvent content was 41.9%.

1. Introduction

Threonine contains two chiral centres and exists as four stereoisomers (L-, L-*allo*-, D- and D-*allo*-threonine). The interconversion of several β -hydroxy- α -amino acids (e.g. threonine) and glycine plus the corresponding aldehydes (e.g. acetaldehyde) is catalyzed by threonine aldolases (Liu, Dairi *et al.*, 2000). In general, threonine aldolases are classified into L- and D-type enzymes according to their stereospecificity at the α -carbon. Depending on their stereospecificity at the β -carbon of threonine, L-type threonine aldolases can be further classified into three types (Dückers *et al.*, 2010): L-threonine-specific and L-*allo*-threonine-specific enzymes [L-threonine aldolase (EC 4.1.2.5) and L-*allo*-threonine aldolase (EC 4.1.2.49), respectively], and low-specificity L-threonine aldolase (EC 4.1.2.48), which accepts both L-threonine and L-*allo*-threonine as substrates. Regarding the D-type enzymes, only low-specificity D-threonine aldolases (DTAs; EC 4.1.2.42) have been found to date (Fesko, 2016).

DTA is considered to be a powerful tool for catalyzing the cleavage or formation of C–C bonds in synthetic organic chemistry (Dückers *et al.*, 2010; Kataoka *et al.*, 2016). The cleavage reaction is important for the chiral resolution of β -hydroxy- α -amino acid intermediates that are necessary for the production of thiamphenicol, an antibiotic, and L-*threo*-3,4-dihydroxyphenylserine, a therapeutic drug for Parkinson's disease (Liu *et al.*, 1999; Liu, Odani *et al.*, 2000). Moreover, the synthesis reaction results in the production of various useful β -hydroxy- α -amino acids that are active pharmaceutical ingredients used in drug development (Goldberg *et al.*, 2015).



© 2017 International Union of Crystallography

The enzymatic properties of DTA in several bacteria (*e.g.* *Arthrobacter* sp. DK-38) and in the green alga *Chlamydomonas reinhardtii* have been studied in detail. For example, these studies revealed that DTA requires pyridoxal 5'-phosphate (PLP) and several divalent metal cations, such as manganese ions, for catalysis (Kataoka *et al.*, 1997; Hirato *et al.*, 2016). The bacterial DTA from *Arthrobacter* sp. DK-38 was significantly inhibited by thiol reagents, suggesting that a cysteine residue exists in the active centre of the enzyme. However, thiol reagents had no effect on the eukaryotic DTA from *C. reinhardtii* (CrDTA). Furthermore, the turnover number of CrDTA using D-*allo*-threonine as a substrate was sixfold higher than that with D-threonine, although there was little difference in specific activity between D-threonine and D-*allo*-threonine as substrates for bacterial DTAs (Liu *et al.*, 1998; Liu, Odani *et al.*, 2000). The amino-acid sequence of CrDTA had comparatively low sequence identity to *Alcaligenes xylosoxidans* DTA (40% sequence identity), whereas the bacterial DTA from *A. xylosoxidans* showed high sequence identity to another bacterial DTA from *Arthrobacter* sp. (91% sequence identity). These results suggest that structural information on CrDTA may be helpful in generating strictly stereoselective D- or D-*allo*-threonine aldolases using rational protein design.

The recent publication of the crystal structure of a bacterial DTA from *A. xylosoxidans* identified a metal-binding site in the active site, which was consistent with previous observations that divalent metal ions are essential for DTA activity (PDB entry 4v15; Uhl *et al.*, 2015). However, the current limited structural information on DTAs makes it difficult to understand the structural differences between bacterial and

Table 1

Macromolecule-production information.

Source organism	<i>C. reinhardtii</i> NIES-2237
DNA source	Synthetic (codon-optimized DNA for <i>E. coli</i> expression)
Forward primer	None
Reverse primer	None
Cloning vector	pUC57
Expression vector	pET-41b(+)
Expression host	<i>E. coli</i> BL21 (DE3)
Complete amino-acid sequence of the construct produced	MRALVSKARLAHSVGGRASQATRCAATISASRAP-AHLGDALHDVDTPALILDLDADFDRNCEKLGVMAGFPGVAVRPHAKAHKCAEVARRQLQLLGA-KVCCQKVEAEAMAEGGVSLLLLSNEVIAPRK-IDRLVGLAAAGARVGVCYEREDNLRQLNAAAA-ARGTHLDVLVELNVGQDRCVNSADEVVQLAR-AAAGLDNVRFAGIQAYHGLQHVRDPRDRAQR-VGVVGRARAARDALKAAGLPCDVTGGGTGT-YRVEAASGVFTEVQPGSFADADYARNLQED-GGVGEWEQSLWVLTQVMSVTPARGLAVVDAGT-KAVSLDSGPPRLPPAFEAAYGTMMYEGSGGDE-HGKLMWPQAYQLPMSLPEVGSLLLLQPQHCD-PTVNLVDLVAARRQGGQGGVGDGWRVEAV-WPIRGRGPGQ

eukaryotic DTAs and to develop stereoselective D- or D-*allo*-threonine aldolases. Thus, more information on the crystal structure of DTA needs to be obtained in order to solve this problem. Here, we report the key steps, such as expression, purification, crystallization and preliminary X-ray analysis, in the structural characterization of CrDTA.

2. Materials and methods

2.1. Macromolecule production

2.1.1. Gene expression of CrDTA. The gene encoding CrDTA with codons optimized for expression in *Escherichia coli* was digested with NdeI and XhoI, and the resulting fragment was ligated into the plasmid vector pET-41b(+), previously digested with the same restriction enzymes, to construct the expression vector pCrDTA (Hirato *et al.*, 2016). The plasmid vector was transferred into *E. coli* BL21 (DE3) competent cells. Single cell clones were selected from Luria-Bertani (LB) plates containing 25 µg ml⁻¹ kanamycin. The clone was cultured in LB medium containing 25 µg ml⁻¹ kanamycin for 16 h at 298 K and then harvested by centrifugation (8000g, 10 min) and stored at 193 K until use.

2.1.2. Purification of CrDTA. *E. coli* cells expressing CrDTA were suspended in 100 mM Tris-HCl buffer pH 8.0 containing 50 µM PLP and 1 mM phenylmethylsulfonyl-fluoride and disrupted by sonication at 80 W for 80 cycles of 30 s followed by cooling for 30 s. After centrifugation, the cell-free extract was fractionated by ammonium sulfate precipitation (25–60% saturation). The enzyme fraction was resuspended in 50 mM Tris-HCl buffer pH 8.0 containing 20 µM PLP and dialyzed in the same buffer. The enzyme solution was centrifuged and applied onto a HiTrap DEAE FF column equilibrated with 50 mM Tris-HCl buffer pH 8.0 containing 20 µM PLP and eluted with a linear gradient of 0–500 mM NaCl in the same buffer at a flow rate of 1 ml min⁻¹. The active fractions were collected and analyzed by SDS-PAGE (Fig. 1) and enzyme assay. Enzymatic activity was

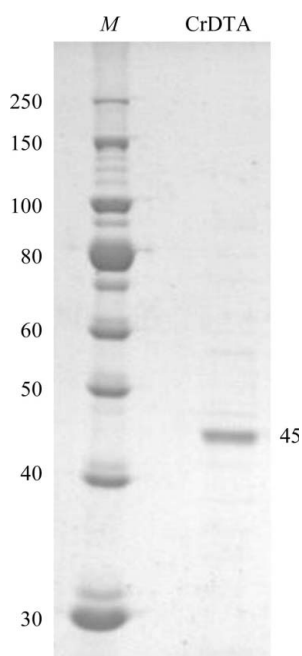


Figure 1
SDS-PAGE of recombinant CrDTA produced in *E. coli* after purification. Purified protein (0.6 µg) was analyzed on a 10% gel. Lane M contains molecular-mass marker (labelled in kDa). The gel was visualized with Coomassie Brilliant Blue.

Table 2
Crystallization.

Method	Hanging-drop vapour diffusion
Plate type	24-well plates
Temperature (K)	295
Protein concentration (mg ml ⁻¹)	7.8
Buffer composition of protein solution	20 mM Tris-HCl pH 8.0, 20 μM PLP, 100 μM MnCl ₂
Composition of reservoir solution	24% PEG 1540, 20% 2-methyl-2,4-pentanediol, 0.2 M magnesium nitrate
Additive solution	50 mM DL-2,3-diaminopropionic acid
Volume and ratio of drop	5 μl (2:2:1 protein:reservoir:additive solution)
Volume of reservoir (μl)	100

determined for each fraction using the coupling method with yeast alcohol dehydrogenase (Liu *et al.*, 1998). The active fractions were pooled and dialyzed against 20 mM Tris-HCl buffer pH 8.0 containing 20 μM PLP and 100 μM MnCl₂. The purified protein was concentrated to 10–20 mg ml⁻¹ using an Amicon Ultra-15 30K centrifugal filter (Millipore, USA) for use in crystallization. Details of macromolecule production are listed in Table 1. The concentration of protein was determined by the Bradford assay (Bradford, 1976) after each purification step.

2.2. Crystallization

Crystallization experiments were performed in 24-well plates at 295 K using the hanging-drop vapour-diffusion method. To screen for crystals of CrDTA, the protein was concentrated to 11 mg ml⁻¹. 2 μl protein solution was mixed with an equal volume of reservoir solution and equilibrated against 100 μl reservoir solution. Initial crystallization screening was performed using three commercial crystallization screens from Hampton Research (Crystal Screen, Crystal Screen 2 and PEG/Ion) and a modified PEG/Ion kit using PEG 1540 as precipitant. Crystals were obtained under several conditions, and the best crystal was obtained using the modified PEG/Ion kit [0.2 M magnesium nitrate, 20% (w/v) PEG 1540] in 9 d. For optimization, the concentration of the crystallization reagent, the pH and the type of the buffer

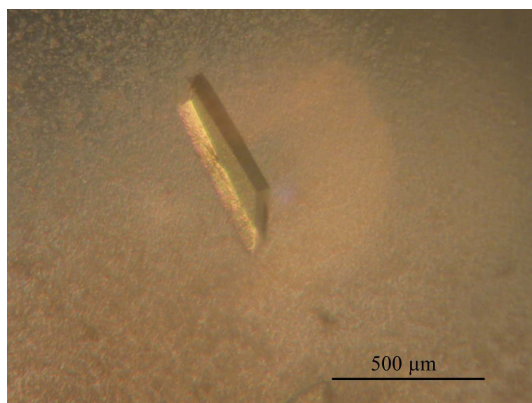


Figure 2
Crystal of CrDTA obtained by the hanging-drop method at 295 K in 24% PEG 1540, 20% 2-methyl-2,4-pentanediol, 0.2 M magnesium nitrate. The scale bar is 500 μm in length.

Table 3
Data collection and processing.

Values in parentheses are for the outer shell.	
Diffraction source	NW-12A, KEK PF-AR
Wavelength (Å)	1.00000
Temperature (K)	95
Detector	ADSC Quantum 210r
Crystal-to-detector distance (mm)	214
Rotation range per image (°)	0.25
Total rotation range (°)	135
Exposure time per image (s)	1
Space group	<i>P</i> 1
<i>a</i> , <i>b</i> , <i>c</i> (Å)	64.79, 74.10, 89.94
α , β , γ (°)	77.07, 69.34, 71.93
Mosaicity (°)	0.43
Resolution range (Å)	42.28–1.85 (1.95–1.85)
Total No. of reflections	181300
No. of unique reflections	111548
Completeness (%)	88.6 (91.3)
Multiplicity	1.6 (1.6)
$\langle I/\sigma(I) \rangle$	9.2 (3.0)
<i>R</i> _{int}	0.062 (0.201)
Overall <i>B</i> factor from Wilson plot (Å ²)	20.0

system were varied, along with the addition of various alcohols and competitive inhibitors, and the hanging drops were set up with 1 μl 50 mM DL-2,3-diaminopropionic acid, which is a substrate analogue of the enzyme, as the additive solution. Crystals suitable for X-ray diffraction were finally harvested within 13 d (Fig. 2). Details of the final crystallization process are listed in Table 2.

2.3. Data collection and processing

X-ray diffraction data were collected from the crystal at a wavelength of 1.00000 Å using an ADSC Quantum 210r CCD detector on beamline NE-12A of the Photon Factory-Advanced Ring (KEK PF-AR), Tsukuba, Japan. A total of 540 images were collected at a crystal-to-detector distance of 214 mm with an oscillation range of 0.25° and an exposure time of 1 s per image. The diffraction data were processed with *XDS* (Kabsch, 2010), *POINTLESS* (Evans, 2006) and *SCALA* (Evans, 2006) within the *CCP4* package (Winn *et al.*, 2011). Data-collection and processing statistics are summarized in Table 3.

3. Results and discussion

Recombinant CrDTA protein expressed in *E. coli* was purified to homogeneity *via* ammonium sulfate fractionation and anion-exchange chromatography. During DEAE-Sepharose chromatography, the protein was eluted at 100–300 mM NaCl, with the peak being at approximately 187 mM. The protein yield was 1.8 mg from a 1 l LB medium culture. SDS-PAGE analysis with Coomassie Brilliant Blue staining identified the purified protein as a single band of approximately 45 kDa, which corresponds to the calculated molecular mass of the recombinant CrDTA monomer (Fig. 1). The protein band on the SDS-PAGE was analyzed using a protein sequencer; the N-terminal sequence of the protein band was identical to that deduced from the CrDTA gene (Hirato *et al.*, 2016).

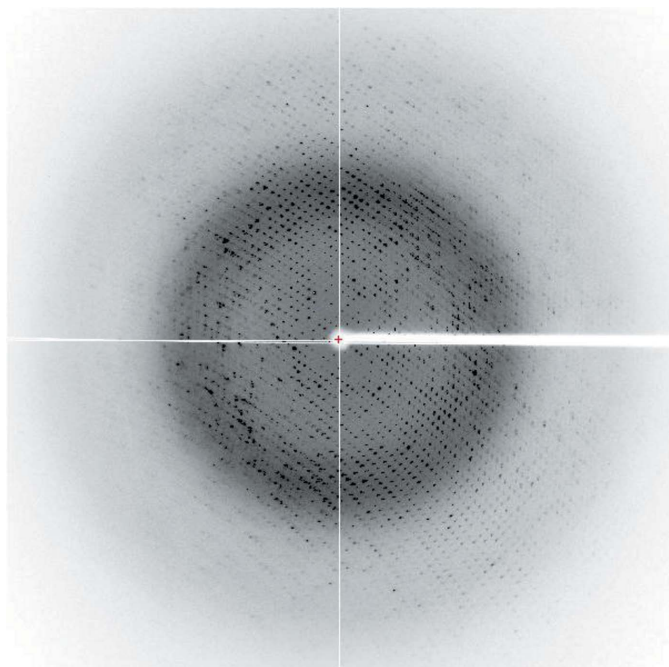


Figure 3
X-ray diffraction image of a CrDTA crystal.

In the initial crystallization screening, clusters of plate-shaped crystals appeared under conditions using PEG 4000 and 2-propanol. The condition was optimized to produce single crystals, and rod-shaped crystals were obtained when a reservoir solution consisting of 24% (*w/v*) PEG 1540, 20% (*v/v*) 2-methyl-2,4-pentanediol, 0.2 *M* magnesium nitrate was used (Fig. 2). A crystal diffracting to a resolution limit of 1.85 Å was finally obtained (Fig. 3). Analysis of the diffraction pattern showed that the crystal belonged to space group *P*1, with unit-cell parameters $a = 64.79$, $b = 74.10$, $c = 89.94$ Å, $\alpha = 77.07$, $\beta = 69.34$, $\gamma = 71.93^\circ$. Assuming the presence of four molecules per asymmetric unit, the calculated Matthews coefficient was $2.12 \text{ \AA}^3 \text{ Da}^{-1}$ (Matthews, 1968), giving an estimated solvent content of 41.9%.

The structure was solved by the molecular-replacement method using *MOLREP* (Vagin & Teplyakov, 2010) with the structure of DTA from *A. xylosoxidans* (PDB entry 4v15), which shares 40% identity with CrDTA, as a search model (Uhl *et al.*, 2015). The results of molecular replacement

showed a clear solution. The *R* factor after an initial round of rigid-body refinement was 49.36%. The crystal contained two dimers per asymmetric unit. The molecular mass of the purified enzyme was determined *via* gel filtration to be 60 kDa (Hirato *et al.*, 2016), suggesting that CrDTA exists in a monomer–dimer equilibrium. Previous studies indicated that the bacterial DTAs from *A. xylosoxidans* and *Arthrobacter* sp. were active as monomers (Liu, Odani *et al.*, 2000; Kataoka *et al.*, 1997), but the crystal structure of DTA from *A. xylosoxidans* was predicted to be a stable dimer in solution (Uhl *et al.*, 2015). Our results indicate that the assembly of CrDTA molecules was similar to that of bacterial DTAs. Structural analysis and refinement are now in progress.

References

- Bradford, M. M. (1976). *Anal. Biochem.* **72**, 248–254.
- Dücker, N., Baer, K., Simon, S., Gröger, H. & Hummel, W. (2010). *Appl. Microbiol. Biotechnol.* **88**, 409–424.
- Evans, P. (2006). *Acta Cryst.* **D62**, 72–82.
- Fesko, K. (2016). *Appl. Microbiol. Biotechnol.* **100**, 2579–2590.
- Goldberg, S. L., Goswami, A., Guo, Z., Chan, Y., Lo, E. T., Lee, A., Truc, V. C., Natalie, K. J., Hang, C., Rossano, L. T. & Schmidt, M. A. (2015). *Org. Process Res. Dev.* **19**, 1308–1316.
- Hirato, Y., Tokuhisa, M., Tanigawa, M., Ashida, H., Tanaka, H. & Nishimura, K. (2016). *Phytochemistry*, <https://doi.org/10.1016/j.phytochem.2016.12.012>.
- Kabsch, W. (2010). *Acta Cryst.* **D66**, 125–132.
- Kataoka, M., Ikemi, M., Morikawa, T., Miyoshi, T., Nishi, K., Wada, M., Yamada, H. & Shimizu, S. (1997). *Eur. J. Biochem.* **248**, 385–393.
- Kataoka, M., Miyakawa, T., Shimizu, S. & Tanokura, M. (2016). *Appl. Microbiol. Biotechnol.* **100**, 5747–5757.
- Liu, J.-Q., Dairi, T., Itoh, N., Kataoka, M., Shimizu, S. & Yamada, H. (1998). *J. Biol. Chem.* **273**, 16678–16685.
- Liu, J.-Q., Dairi, T., Itoh, N., Kataoka, M., Shimizu, S. & Yamada, H. (2000). *J. Mol. Catal. B Enzym.* **10**, 107–115.
- Liu, J.-Q., Odani, M., Dairi, T., Itoh, N., Shimizu, S. & Yamada, H. (1999). *Appl. Microbiol. Biotechnol.* **51**, 586–591.
- Liu, J.-Q., Odani, M., Yasuoka, T., Dairi, T., Itoh, N., Kataoka, M., Shimizu, S. & Yamada, H. (2000). *Appl. Microbiol. Biotechnol.* **54**, 44–51.
- Matthews, B. W. (1968). *J. Mol. Biol.* **33**, 491–497.
- Uhl, M. K., Oberdorfer, G., Steinkellner, G., Riegler-Berket, L., Mink, D., van Assema, F., Schürmann, M. & Gruber, K. (2015). *PLoS One*, **10**, e0124056.
- Vagin, A. & Teplyakov, A. (2010). *Acta Cryst.* **D66**, 22–25.
- Winn, M. D. *et al.* (2011). *Acta Cryst.* **D67**, 235–242.